Fluorescence Dequenching Kinetics of Single Cell-Cell Fusion Complexes

Yi-der Chen, Robert J. Rubin, and Attila Szabo
Laboratory of Chemical Physics, National Institute of Diabetes, Digestive and Kidney Diseases, National Institutes of Health, Bethesda, Maryland 20892 USA

ABSTRACT In an earlier paper which models the cell-cell (or virus-cell) fusion complex as two partial spherical vesicles joined at a narrow neck (Rubin, R. J., and Yi-der Chen. 1990. *Biophys. J.* 58:1157–1167), the redistribution by diffusion of lipid-like molecules through the neck between the two fused cell surfaces was studied. In this paper, we extend the study to the calculation of the kinetics of fluorescence increase in a single fusion complex when the lipid-like molecules are fluorescent and self-quenching. The formalism developed in this paper is useful in deducing fusion activation mechanisms from cuvette fluorescence measurements in cell-cell fusion systems. Two different procedures are presented: 1) an exact one which is based on the exact local density functions obtained from diffusion equations in our earlier study; and 2) an approximate one which is based on treating the kinetics of transfer of probes between the two fused cells as a two-state chemical reaction. For typical cell-cell fusion complexes, the fluorescence dequenching curves calculated from the exact and approximate procedures are very similar. Due to its simplicity, the approximate method should be very useful in future applications. The formalism is applied to a typical cell-cell fusion complex to study the sensitivity of dequenching curves to changes in various fusion parameters, such as the radii of the cells, the radius of the pore at the fusion junction, and the number of probes initially loaded to the complex.

INTRODUCTION

The first steps in the infection of animal cells by enveloped virus are the binding and fusion of the cell and viral membranes (1, 2). It is known that the membrane fusion event is mediated by viral spike glycoproteins and that these proteins undergo a number of "activation" reactions, such as the binding of hydrogen ions (H^+), conformational changes, aggregation reactions, etc., before the membranes coalesce to form a junction pore. Recently, self-quenching lipid-like R-18 (octadecyl rhodamine B chloride) molecules have been used extensively to study the kinetics of fusion activation of cells with enveloped viruses or with hemagglutinin-expressed cells (3–9). The method is based on the self-quenching property of this dye: the intensity of fluorescence increases when the density of the dye decreases and vice versa. Thus, upon fusion of R-18-containing membranes with membranes devoid of the probe, the total fluorescence of the system increases due to diffusion and redistribution of the dye between the two membranes. In these experiments, kinetic properties of fusion activation reactions can be studied quantitatively by measuring the time-dependent fluorescence signal. The technique has been used extensively in cuvette experiments in which the fluorescence change of a population of fused cells is measured (3–9). Recently, the measurement of fluorescence dequenching in single cell-cell fusion complexes mediated by influenza hemagglutinin has been reported (10).

In general, the time dependence of the fluorescence intensity of a fusion system in cuvette experiments contains two kinetic components: (i) the fusion activation reactions leading to the coalescence of the membranes and the opening of the pore(s); and (ii) the redistribution of the probes between the coalesced membranes. Thus, the dequenching kinetic data measured in cuvette experiments accurately reflects the kinetics of fusion activation reactions only if the redistribution reaction of the probes is not rate-limiting (11). When the rates of the two kinetic processes are comparable, the evaluation of the separate rate constants is not straightforward (11). The redistribution of R-18 has been assumed to be fast (not rate-limiting) in many fusion studies (6–9).

To test the validity of this assumption, we carried out a theoretical study (12) (hereafter referred to as paper I) of the redistribution by diffusion of lipid-like molecules between the membranes of two coalesced spherical vesicles (see Fig. 1). The time-dependent spatial density functions of the probes on the two vesicles were obtained by solving the time-dependent diffusion equation of the composite system. The kinetic behavior of probe redistribution was then evaluated from these density functions. It was found that the time scale of redistribution of lipid-like dyes was more sensitive to changes in the radii of the fusing cells than to changes in the radius of the pore at the junction. Thus, the redistribution half-time of lipid dye is rather long (~150 s) in typical cell-

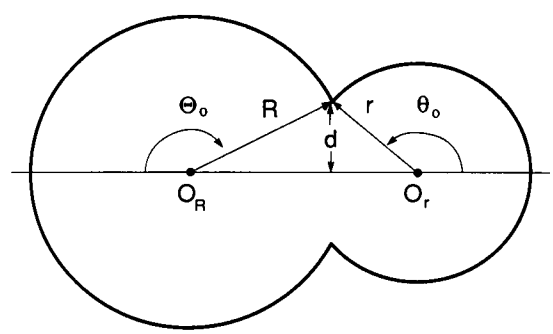

FIGURE 1 Schematic drawing of the cross section of a fusion complex. R and r are the radii of the two fused cells. d is the radius of the pore at the fusion junction. The direction of increase of the polar angles, θ and Θ, are indicated by the circular arrows.

Received for publication 20 July 1992 and in final form 12 April 1993.

0006-3495/93/07/325/09 $2.00

cell fusion (such as between human erythrocyte and Gp4f cells), although it is short (~0.02 s) in virus-cell fusion. Consequently, the cuvette experiment, in which the rate of fluorescence change of a population of fusion complexes is measured, provides a convenient means for studying fusion activation mechanisms in the case of virus-cell fusion, but not in the case of cell-cell fusion. In other words, the degree of dequenching in a cuvette experiment directly reflects the fraction of fused complexes in the virus-cell case, but not in the cell-cell case. To deduce the kinetics of fusion activation reactions from cuvette fluorescence measurements for the cell-cell fusion case, the kinetic properties of fluorescence dequenching of single cell-cell fusion complexes in the system are required (11). Thus, we thought it worthwhile to develop a theoretical formalism for calculating the fluorescence of a single cell-cell fusion complex for the model studied in I.

Recently, measurements of R-18 fluorescence in single cell-cell fusion complexes have been reported by Kaplan et al. (10). As schematically shown in Fig. 2, a typical fluorescence record of a single cell-cell fusion complex consists of a phase with no change in fluorescence (the duration of this phase is called the lag time) followed by a phase with an exponential-like rise of fluorescence. The distribution of lag times in phase 1 is related to the mechanisms of the fusion activation reactions; and the fluorescence increase in phase 2 is related to the diffusion and dequenching of probes after fusion. One interesting finding of Kaplan et al. (10) in studying single fusion complexes between human RBC (red blood cell) and hemagglutinin-expressed Gp4f cells is that the half-time for increase of fluorescence in phase 2 varies considerably from one complex to the next. That is, the half-time for dequenching of R-18 molecules after membrane fusion is not uniform among the fusion complexes. It is known that some parameters of the system are difficult to control in the experiment. For example, the total number of R-18 molecules loaded to each RBC cell initially is not easily controlled; the size of the pore at the fusion junction may vary from complex to complex, because the number of the pore-inducing hemagglutinin molecules expressed in each Gp4f cell is not expected to be the same; the cell size of either RBC or Gp4f cells may not be uniform, etc. Any or all of these factors could be the cause of the observed wide distribution of R-18 dequenching rates. To study how these factors affect the fluorescence dequenching kinetics also requires a theoretical formalism for the calculation of fluorescence dequenching in a single fusion complex.

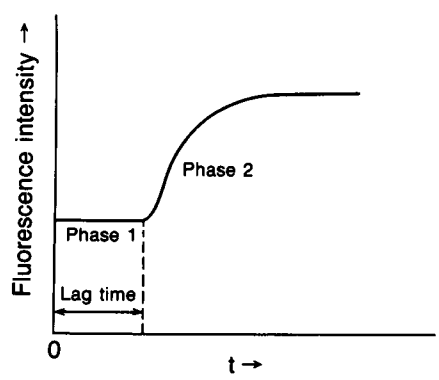

FIGURE 2 Schematic drawing of the total fluorescence intensity profile, $F(t)$, of a single fusion complex caused by diffusion of self-quenching probes from the probe-loaded r cell surface to the probe-void R cell. Fusion activation occurs at $t = 0$. The "lag time" is the time between the onset of fusion activation and the start of the increase of the fluorescence intensity.

Thus, in the Theory and Calculation of Fluorescence Dequenching section we first develop a general formalism for the calculation of fluorescence dequenching in a single fusion complex based on the model and results of paper I. The formalism is called "exact," because exact local time-dependent densities of probes obtained in paper I are used in the calculation procedure. Numerical calculations of fluorescence dequenching curves using this formalism are computer-intensive. Therefore, we present, under An Approximate Method for Calculating $X(t)$, an "approximate" formalism based on "averaged" probe densities on the two cell surfaces. That is, the surface density of probes is assumed to be uniform on each cell at any time, and the kinetics of transfer of probes between the two fused cells is treated as a two-state chemical reaction with first-order rate constants that are determined by the dimensions of the fusion complex. The formula obtained for fluorescence dequenching is very simple and easy to evaluate. Under Illustrative Calculations, we present some illustrative sample calculations from both the exact and the approximate formalisms. The purpose is twofold: 1) to show that, for typical cell-cell fusion complexes, the difference in calculated fluorescence dequenching between the two formalisms is very small; and 2) to study how the fluorescence dequenching kinetics is affected by the dimensions of the fusion complex and other system parameters.

THEORY AND CALCULATION OF FLUORESCENCE DEQUENCHING

The diffusion or redistribution of self-quenching lipid-like dye molecules from the dye-loaded cell surface to the unloaded is assumed to be the sole cause of fluorescence increase in a single fusion complex. As shown in Fig. 1, a fusion complex is represented by two coalesced spherical cells of radii r and R with a single pore of radius d at the fusion junction. Initially, self-quenching dye molecules are loaded evenly on the surface of the r cell at surface density n_0. At time $t = 0$ they start to diffuse to the R cell, resulting in dequenching and an increase in the total fluorescence of the complex. Throughout the redistribution process, the surface density maintains its cylindrical symmetry.

As discussed before (11), we assume that the fluorescence intensity of self-quenching fluorophores at any given point on the surface of a fusion complex at any given time is completely determined by the local instantaneous density of fluorophores at that point. In other words, diffusion and redistribution of the fluorophores on the membrane are considered to be slow compared to the excitation, de-excitation, and quenching reactions of the fluorophores.

Given an initial uniform surface density of fluorophores on the r cell (or the R cell) of the fusion complex in Fig. 1, the local surface density on each cell at time t (the time after the membranes are fused) is a function of only one polar angle, due to axial symmetry of the system. Let the densities on the r cell and the R cell be, respectively, $n(\theta,t)$ and $N(\Theta,t)$, where θ and Θ

are the polar angles shown in Fig. 1. Explicit formulas for these densities are given in Eqs. 7 and 8 of paper I. Each polar angle is zero at the pole opposite the fusion junction and increases to the values θ_o and Θ_o at the junction. The values of θ_o and Θ_o are determined by the radius of the pore at the fusion junction and the radii of the two cells as $d = r \sin \theta_o = R \sin \Theta_o$.

In terms of the two local surface densities, the total fluorescence intensity of the fusion complex can be written as

$$F(t) = F_r(t) + F_R(t) \tag{1}$$

where

$$F_r(t) = 2\pi r^2 \int_0^{\Theta_0} n(\Theta,t) f[n] \sin \theta \, d\theta \tag{2}$$

and

$$F_R(t) = 2\pi R^2 \int_0^{\Theta_0} N(\Theta,t) f[N] \sin \Theta \, d\Theta \tag{3}$$

and where $f[n]$ and $f[N]$ are the "specific" fluorescences (i.e., the fluorescence intensity per molecule) of probes at density n and N, respectively. Note that the specific fluorescence intensity of a probe depends on its density, because the probes are self-quenching.

We next define the *degree of dequenching*, a normalized total fluorescence intensity, which is more useful in interpreting experiments:

$$X(t) = [F(t) - F(0)]/[F(\infty) - F(0)] \tag{4}$$

where $F(0)$ and $F(\infty)$ are, respectively, the initial and the final equilibrium fluorescence intensities of a fusion complex. The degree of dequenching, $X(t)$, increases from 0 to 1 as t increases from 0 to ∞.

At $t = \infty$, fluorophores are uniformly distributed on the surface of the complex. Thus, the surface densities on the r cell and the R cell are equal and are related to the initial ($t = 0$) density on the r cell n_o as

$$N_\infty = n_\infty = n_o A_r/(A_r + A_R) \tag{5}$$

where A_r and A_R are, respectively, the partial areas of the r and the R cells as follows:

$$A_r = 2\pi r^2(1 - \cos \theta_o), \tag{6}$$

$$A_R = 2\pi R^2(1 - \cos \Theta_o). \tag{7}$$

Thus, the total fluorescence intensities of a fusion complex at $t = 0$ and ∞ can be shown to be

$$F(0) = n_o f[n_o] A_r \tag{8}$$

and

$$F(\infty) = n_\infty f[n_\infty](A_r + A_R) = n_o f[n_\infty] A_r. \tag{9}$$

The specific fluorescence in Eqs. 2 and 3 is expected, on theoretical grounds, to have the following dependence on density,

$$f[n] = f_d/(1 + \kappa n) \tag{10}$$

where κ is a proportionality constant and f_d is the specific fluorescence of the probes at infinite dilution ($n = 0$; no quenching). Recent fluorescence quenching experiments by Aroeti and Henis (13) with R-18, both in native Sendai virions and in vesicles made from lipid extracts of the virus, exhibit behavior which is consistent with the form of $f[n]$ in Eq. 10. In other experiments, Hoekstra et al. (3) have found that the specific fluorescence of R-18 molecules on pure lipid vesicles can be fit empirically by the linear function

$$f[n] = f_d(1 - \kappa n) \tag{11}$$

if the surface density is less than 7%. In many fusion experiments (4–9), this linear function is used in the interpretation of the experiments. It is clear that the empirical form in Eq. 11 can be obtained from Eq. 10 by truncating its expansion in powers of κn after the linear term, a valid operation provided that $\kappa n \ll 1$ (however this condition is not met by the nonlinear quenching systems studied by Aroeti and Henis (13), see below). To be general, both expressions for the specific fluorescence will be considered in this study.

With the specific fluorescence of probes given in Eqs. 10 or 11 and explicit formulas for $n(\theta,t)$ and $N(\Theta,t)$ given in Eqs. 7 and 8 of paper I, the degree of dequenching in Eq. 4 can be evaluated by carrying out the integration in Eqs. 2 and 3. It is obvious that the total fluorescence of a fusion complex, $F(t)$, is linearly proportional to f_d, the limiting specific fluorescence of R-18 at zero density. As a result, the degree of dequenching $X(t)$ defined in Eq. 4 is independent of f_d. With Eqs. 7 and 8 of paper I, it can be shown that $X(t)$ is also independent of the values of n_o and κ, if the linear specific fluorescence function, Eq. 11, is used. In the nonlinear specific fluorescence case, $X(t)$ depends on the product $n_o\kappa$.

The calculation of $X(t)$ using the exact $n(\theta,t)$ and $N(\Theta,t)$ in Eqs. 7 and 8 of paper I (referred to as the exact formalism) involves numerical integration of complicated hypergeometric functions and is therefore not very practical. In the next section, we present a useful approximate formalism for the calculation of $X(t)$ based on approximate local probe densities.

AN APPROXIMATE METHOD FOR CALCULATING $X(t)$

If the radius of the pore at the fusion junction is sufficiently small compared to the radii of the fused cells, the redistribution half-time of fluorophores on each cell surface in Fig. 1 is expected to be significantly less than the transfer half-time of fluorophores across the junction; and consequently the surface density gradient of fluorophores will be very small on each cell surface, except in the immediate vicinity of the junction. In this approximate method, we assume that quasiequilibrium has been achieved on each cell at any given time so that the fluorophores are *uniformly* distributed on each cell surface. Thus, the basic idea which underlies our approximate method is to replace the two local densities, $n(\theta,t)$ and $N(\Theta,t)$, which appear explicitly in the total fluorescence intensity, Eqs. 2 and 3, by *uniform* quasiequilibrium densities on each cell. These quasiequilibrium densities are defined as the total number of fluoropohores on a cell divided by its surface area.

When the junction between the fused cells is small, the probability of finding the probes in this region is clearly also small. Thus, the fusion junction acts as an "entropic" barrier (14, 15) to the transfer of probes. With the assumption of a high barrier between the two fused cells (or equivalently, a small junction), the dynamics of the transfer of fluorophores between the surfaces of the two fused cells can be described accurately by simple chemical kinetics. Let $n_T(t)$ and $N_T(t)$ be the total *number* (not the density!) of fluorophores on the surfaces of the r and R cells, respectively, at time t. These satisfy the rate equations

$$dn_T(t)/dt = -k_{r\to R} n_T(t) + k_{R\to r} N_T(t) \tag{12}$$

$$dN_T(t)/dt = k_{r\to R} n_T(t) - k_{R\to r} N_T(t) \tag{13}$$

where $k_{r\to R}$ and $k_{R\to r}$ are the first-order rate constants describing the transfer of fluorophores between the two cells. Since R-18 is only loaded to the r cell initially and is

conserved, we have

$$N_T(t) = n_T(0) - n_T(t). \tag{14}$$

Then, Eqs. 12 and 13 can be solved as

$$n_T(t) = n_T(\infty) + [n_T(0) - n_T(\infty)]e^{-t/\tau} \tag{15}$$

$$N_T(t) = [n_T(0) - n_T(\infty)][1 - e^{-t/\tau}] \tag{16}$$

where

$$n_T(0) = n_o A_r \tag{17}$$

$$n_T(\infty) = n_\infty A_r = n_o A_r^2/(A_r + A_R) \tag{18}$$

and

$$\tau = (k_{r\to R} + k_{R\to r})^{-1}. \tag{19}$$

Upon replacing the local densities, $n(\theta,t)$ and $N(\Theta,t)$, in Eqs. 2 and 3 by the uniform densities, $n_T(t)/A_r$ and $N_T(t)/A_R$, obtained from Eqs. 15 and 16, respectively, the "approximate" degree of dequenching, $X_{app}(t)$, can be obtained from Eqs. 1–4 as

$$X_{app}(t) = \left\{f[n_T(t)/A_r] - f[n_o] + \left(\frac{A_R}{A_r + A_R}\right)(1 - e^{-t/\tau}) \times (f[N_T(t)/A_R] - f[n_T(t)/A_r])\right\}/(f[n_\infty] - f[n_o]). \tag{20}$$

In the case of the nonlinear specific fluorescence function, Eq. 10, the approximate degree of dequenching reduces after some tedious algebra to

$$X_{app}(t) = \left[1 - \frac{E}{1 + s_o\omega(1 - E)}\right] \times \left[1 + \frac{E}{1 + s_o[\omega + (1 - \omega)E]}\right] \tag{21}$$

where $s_o = \kappa n_o$, $\omega = A_r/(A_r + A_R)$, and $E = \exp(-t/\tau)$.

In the case of the linear specific fluorescence function, Eq. 11, the approximate degree of dequenching is

$$X_{app}(t) = 1 - E^2. \tag{22}$$

As in the exact formalism, the degree of dequenching obtained from this approximate treatment is independent of $n_o\kappa$ if the specific fluorescence is linear.

We are now faced with the problem of relating the phenomenological macroscopic relaxation time τ in Eq. 19 to the microscopic parameters of the fusion complex. We outline two methods for solving this problem in appendices A and B. In Appendix A, we show that τ can be derived directly from the exact formula in paper I for the time-dependent total number of fluorophores in the r cell, $n_T(t)$. Define $\eta(t)$ as the normalized deviation from equilibrium of the total number of probes on the r cell as follows:

$$\eta(t) = [n_T(t) - n_T(\infty)]/[n_T(0) - n_T(\infty)]. \tag{23}$$

Then, $\eta(t)$ is equal to unity at $t = 0$ and decays monotonically to zero at $t = \infty$. Note that this $\eta(t)$ is evaluated in Eq. 14 of paper I and is a sum of exponentials in the time. If the approximate $n_T(t)$ in Eq. 15 is substituted in Eq. 23, we obtain an approximate $\eta(t)$

$$\eta_{app}(t) = e^{-t/\tau} \tag{24}$$

which also has a value of unity at $t = 0$ and decays to zero at $t = \infty$. Note that the area under this $\eta_{app}(t)$ is equal to τ:

$$\tau = \int_0^\infty \eta_{app}(t)\, dt. \tag{25}$$

To express τ in terms of microscopic parameters in a consistent way, we define τ as the area under the exact (multiexponential) relaxation function, $\eta(t)$:

$$\tau = \int_0^\infty \eta(t)\, dt. \tag{26}$$

The derivation of τ using this approach is outlined in Appendix A. The final result is

$$\tau = \frac{1}{D}\left\{\left(\frac{r^2A_R}{A_r + A_R}\right)\left[\frac{1}{\zeta_o}\ln\left(\frac{1}{1 - \zeta_o}\right) - 1\right] + \left(\frac{R^2A_r}{A_r + A_R}\right)\left[\frac{1}{Z_o}\ln\left(\frac{1}{1 - Z_o}\right) - 1\right]\right\} \tag{27}$$

where A_r and A_R are given in Eqs. 6 and 7 and $\zeta_o = (1 - \cos\theta_o)/2$ and $Z_o = (1 - \cos\Theta_o)/2$.

In Appendix B, we show that Eq. 27 can also be derived by establishing an exact correspondence between our diffusion-through-a-constriction model and the well studied, general model of diffusive barrier crossing of particles in a one-dimensional bistable potential (16–18). That is, the transfer of lipid-like probes between the two fused cells in a fusion complex is shown to be mathematically equivalent to the transfer of particles across an "entropic" potential barrier. This approach has a number of appealing features: it places the problem in the general context of chemical kinetics; it by-passes the rather complicated exact time-dependent solution; and it is applicable to other situations (e.g., a more complicated potential) where an exact analytic solution of the time-dependent problem does not exist.

One must note that it is trivial to evaluate τ in Eq. 27. It is shown below that differences between the calculated $X(t)$ curves obtained using the exact densities and the quasiequilibrium densities are very small for both linear and nonlinear specific fluorescence functions. Therefore, our local quasiequilibrium approximation procedure should be very useful for analyzing fluorescence dequenching data in cell-cell fusion experiments.

ILLUSTRATIVE CALCULATIONS

The calculations presented in this section serve three purposes. First, they show that the differences between the

values of the degree of dequenching, $X(t)$, calculated by the exact and the approximate method, are small. As a result, the simpler approximate calculation procedure will be useful in future applications. Second, they show that the mode of quenching of the fluorophores, whether linearly or nonlinearly dependent on the concentration of probes, has a great effect on the values of $X(t)$. Third, they provide a quantitative measure of the effect of changes in various parameters of the fusion system on the kinetics of fluorescence dequenching, such as the sizes of the cells, the size of the pore at the fusion junction, and the number of fluorophores initially loaded to the complex.

Following Kaplan et al. (10), we consider the fusion complex composed of a red blood cell and a Gp4f cell. The typical dimensions of a fusion complex are assumed to be $r = 3.5$ μm, $R = 10$ μm, and $d = 0.05$ μm. The diffusion coefficient of R-18 on both cells is assumed to be fixed at 10^{-8} cm^2/s or 1 μm^2/s. The initial density on the r cell, n_0, is assumed to be less than 7%, with a typical value of 3%. The value of κ is required in the calculation of $X(t)$, if the nonlinear specific fluorescence function, Eq. 10, is used.

We have estimated that the value of κ in Eq. 10 is 2/unit mole% of R-18 from Fig. 1 of Aroeti and Henis (13). The details of our analysis of their data are presented in Appendix C. Thus, if the molar density of R-18 initially loaded to the r cell is 3% (a typical value in most experiments (4–9)), the value of s_0 ($= \kappa n_0$) is equal to 6. In all calculations shown below, κ is set to the value of 2 and n_0 is treated as a variable parameter of the fusion system.

Fig. 3 shows some of the calculated $X(t)$ curves. Both the exact and the approximate methods were used in these calculations. Only the exact results are shown, because the differences between the two calculations were very small (see Fig. 4). Also, both the linear (*left panels*) and the nonlinear (*right panels*) specific fluorescence cases were studied.

The effect of change in pore size on $X(t)$ is shown in Fig. 3, a and a'; while in Fig. 3, b and b', the effect of change in cell size and change in the number of loaded fluorophores (the nonlinear quenching case only) on the degree of dequenching kinetics is illustrated. In general, increasing the pore size increases the rate of dequenching. In contrast, the rate of dequenching decreases when the size of either cell increases. However, for the same percentage change in cell radius, a change in the smaller cell radius has a larger effect on the dequenching rate in case the specific fluorescence function is linear. For the nonlinear-specific fluorescence

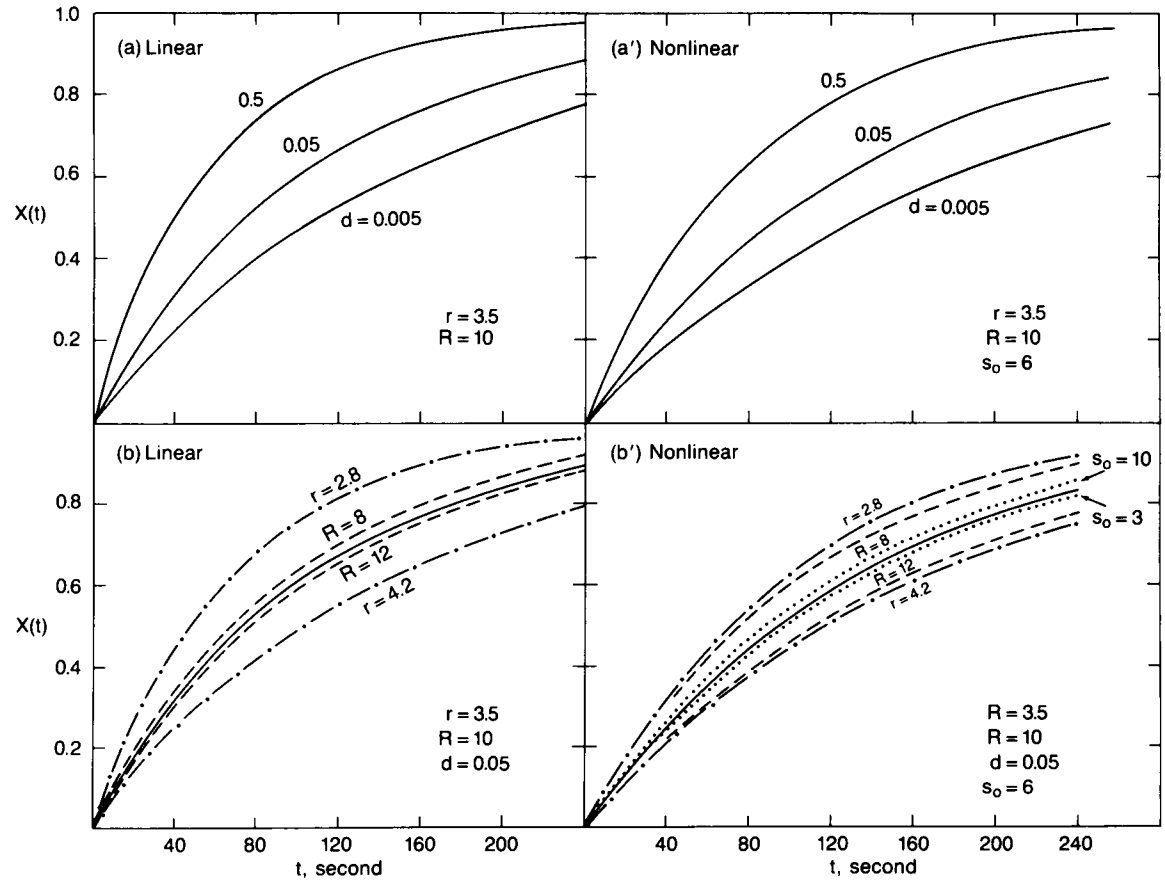

FIGURE 3 The effect of a change of a fusion parameter on the degree of dequenching, $X(t)$. The curves on the left panels (a and b) are calculated with a linear specific fluorescence function; while those on the right (a' and b') are calculated with a nonlinear specific fluorescence. The parameters of a standard fusion complex are chosen as ($r = 3.5$ μm, $R = 10$ μm, $d = 0.05$ μm, and $s_0 = 6$). Each parameter is varied in turn to investigate its effect on the calculated dequenching rate. Each curve is labeled by a parameter if that parameter differs from the standard set.

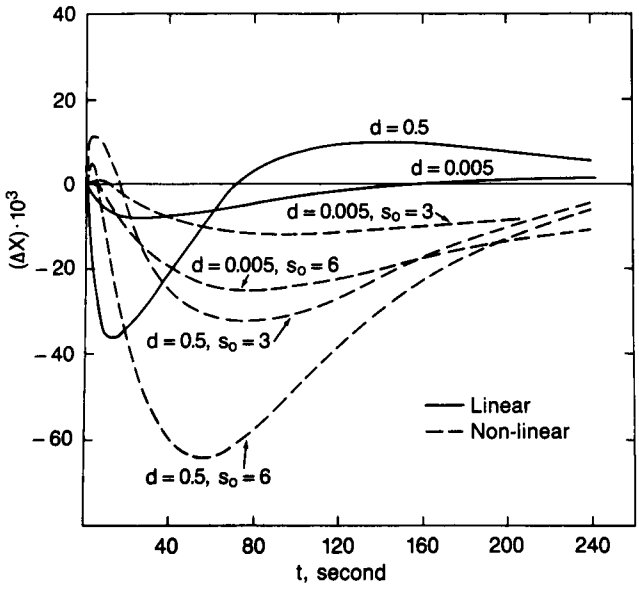

FIGURE 4 Deviations in the calculated $X(t)$ curves between the approximate and the exact methods, $\Delta X = X_{exac}(t) - X_{app}(t)$, at two d values for the standard fusion complex.

case, a change in the size of either cell has about the same effect on the dequenching curve (see the curves indicated with *dashes* and with *dashes* and *dots* in Fig. 3, *b* and *b'*).

In case the specific fluorescence is nonlinear, the dequenching kinetics appears to be insensitive to the initial concentration of fluorophores, n_o (for the linear case, $X(t)$ is independent of n_o). All these phenomena are summarized in Tables 1 and 2, where the dequenching half-times of the curves shown in Fig. 3 are listed.

As can be seen in Fig. 3 and Tables 1 and 2, the values of the rate of fluorescence increase seems to depend greatly on whether the linear or the nonlinear specific fluorescence function is used in the calculation. Specifically, for the same fusion complex, the calculated half-times for the nonlinear case are always larger than for the linear case. Thus, it is important to know the mode of dequenching of the fluorescent probes, before one attempts to correlate the dequenching rate with the dimension of the fusion complex.

TABLE 1 Exact and approximate dequenching half-times calculated using the linear specific fluorescence function (Eq. 11)

r	R	d	t_{exac}	t_{app}
μm	μm	μm	s	s
3.5	10	0.005	109	107
		0.05	74	72
		0.5	38	36
3.5	8	0.05	68	67
	10		74	72
	12		78	75
2.8	10	0.05	48	46
3.5			74	72
4.2			104	101

TABLE 2 Exact and approximate dequenching half-times calculated using the nonlinear specific fluorescence function (Eq. 10)

r	R	d	s_o	t_{exac}	t_{app}
μm	μm	μm		s	s
3.5	10	0.005	3	98	92
			6	95	85
			10	88	75
3.5	10	0.005	6	133	125
		0.05		95	85
		0.5		55	44
3.5	8	0.05	6	74	68
	10			95	85
	12			112	99
2.8	10	0.05	6	71	62
3.5				95	85
4.2				116	106

The difference, $\Delta X = X_{exac}(t) - X_{app}(t)$, calculated for a standard fusion complex is shown in Fig. 4. As can be seen in the figure (also see Tables 1 and 2), the difference between the dequenching curves calculated using the two methods is small at all times for both the linear and nonlinear specific fluorescence functions. However, the difference is larger in the case of the nonlinear specific fluorescence function (Eq. 10). No matter whether the specific fluorescence function is linear or nonlinear, the difference, ΔX, becomes more pronounced when the pore at the fusion junction becomes larger. This is expected, because the surface area-weighted differences in particle density, $n(\theta,t) - n_T(t)/A_r$ and $N(\Theta,t) - N_T(t)/A_R$, become larger when the pore at the fusion junction becomes larger.

DISCUSSION

The purposes of this paper are: (i) to present a procedure for the calculation of the kinetics of fluorescence increase in a single cell-cell fusion complex caused by redistribution of self-quenching lipid-like probes between two fused cells; and (ii) to investigate theoretically how the rate of fluorescence change in a single cell-cell fusion complex is influenced by the physical dimensions of the fusion complex and the number of fluorophores initially loaded to the complex. This is an extension of our previous work (12), in which the rate of redistribution of lipid-like molecules in a fusion complex, not the fluorescence dequenching, was discussed.

As discussed under the Theory and Calculation of Fluorescence Dequenching section, two concentration-dependent forms of specific fluorescence for R-18 have been used in our calculations. The "linear" form in Eq. 11 is based on the finding of Hoekstra et al. (3) that the degree of fluorescence quenching of R-18 molecules in lipid vesicles is linearly proportional to the density or concentration of the probes present in each vesicle. As discussed recently by Aroeti and Henis (13), linear quenching of R-18 is observed in vesicles made of pure lipid molecules; but linear quenching is not observed in native Sendai virions, or in vesicles made of lipids extracted from the virus. As discussed in Appendix C,

their nonlinear quenching data can be fitted nicely by Eq. 10 with a κ value of 2/unit mole%. The main differences between the linear and the nonlinear cases are: (i) The degree of fluorescence dequenching of a fusion complex is independent of the number of probes initially loaded to the complex only in the linear case; and (ii) For typical probe densities (around 3 mole%), the rate of R-18 fluorescence dequenching of the same fusion complex is significantly smaller in the nonlinear case than in the linear case. It is clear from these results that the mode of quenching (or dequenching) of R-18 probes used in fluorescence experiments should be determined before correlating the kinetics of fluorescence change with the structure of the fusion complex. It is interesting to note that, as discussed by Aroeti and Henis (13), it is the lipids of the membrane that determine whether the self-quenching of R-18 is linearly or nonlinearly dependent on the probe concentration.

In general, the exact procedure to calculate the degree of dequenching, $X(t)$, for either linear or nonlinear specific fluorescence, is to use the position- and time-dependent particle density functions obtained in paper I. These density functions consist of infinite series containing hypergeometric functions and are therefore not very practical in numerical calculations. As discussed under An Approximate Method for Calculating $X(t)$, we show that a simpler method can be used which is based on a quasiequilibrium approximation for the local particle density. As shown in Fig. 4 and in Tables 1 and 2, the difference between the degree of dequenching calculated by the exact method and the approximate method is small for typical cell-cell fusion complexes. Since the relaxation time constant τ in this approximate formalism involves only elementary functions, the approximate method is very useful for practical calculations.

Finally, we want to point out that, as shown in Fig. 3 and Tables 1 and 2: (i) the kinetics of fluorescence dequenching of a fusion complex depends on the value of n_o, the initial probe density on the smaller r cell, in case the quenching of fluorescent probes is nonlinearly dependent on the probe concentration. However, under ordinary experimental conditions, the dequenching kinetics is not very sensitive to the value of n_o; (ii) the degree of dequenching reaches its equilibrium value (at $t = \infty$) faster when the pore at the junction becomes larger, or when the sizes of the two fusion cells become smaller; and (iii) for the same percentage change, the rate constant of dequenching is more sensitive to the sizes of the cells of the fusion complex than to the size of the pore at the fusion junction. These results imply that the wide spread in rate constants of normalized dequenching curves as observed by Kaplan et al. (10) probably is not the result of inhomogeneous loading of the probes among the fusion complexes, but the result of inhomogeneous distribution of pore and cell sizes.

APPENDIX A. DERIVATION OF τ USING THE RESULTS OF PAPER I

As discussed under An Approximate Method for Calculating $X(t)$, the value of τ, the relaxation time of a one-exponential approximation to the relaxation function $\eta(t)$, is equal to the area under $\eta(t)$ defined in Eq. 23 and obtained explicitly in Eq. 12 of paper I. Thus, in principle, this area could be obtained by integrating the formula for $\eta(t)$ in Eq. 12 of paper I. But then, an infinite series which must be summed is obtained for τ. A simpler procedure for deriving a useful expression for the area under the relaxation curve $\eta(t)$ is to use the Laplace transform of $\eta(t)$ from which the series in Eq. 12 of paper I was obtained. The Laplace transform of Eq. 23 is

$$\tilde{\eta}(p) = \int_0^\infty \eta(t) e^{-pt}\, dt \tag{A1}$$

$$= \left[\frac{\tilde{n}_T(p)}{n_T(0)} - \frac{1}{p}\frac{n_T(\infty)}{n_T(0)}\right] \Big/ \left[1 - \frac{n_T(\infty)}{n_T(0)}\right] \tag{A2}$$

and the area under the $\eta(t)$ relaxation curve is, from Eq. A1,

$$\lim_{p\to 0} \tilde{\eta}(p) = \int_0^\infty \eta(t)\, dt = \tau \tag{A3}$$

or, from Eq. A2,

$$\tau = \left[1 - \frac{n_T(\infty)}{n_T(0)}\right]^{-1} \lim_{p\to 0}\left[\frac{\tilde{n}_T(p)}{n_T(0)} - \frac{1}{p}\frac{n_T(\infty)}{n_T(0)}\right]. \tag{A4}$$

The expression for $\tilde{n}_T(p)/n_T(0)$ in Eq. A4 follows, from Eqs. A24, A31, and A32 of paper I as

$$\frac{\tilde{n}_T(p)}{n_T(0)} = \frac{1}{p}\left[1 - \frac{{}_2F_1[a, 1-a; 2; \zeta_o]}{\mathcal{F}(p, \zeta_o, Z_o)}\right] \tag{A5}$$

where ${}_2F_1[\ldots]$ is the hypergeometric function

$${}_2F_1[\alpha, \beta; \gamma; \chi] = 1 + \frac{\alpha\beta}{\gamma \times 1}\chi + \frac{\alpha(\alpha+1)\beta(\beta+1)}{\gamma \times (\gamma+1) \times 1 \times 2}\chi^2 + \ldots \tag{A6}$$

and from Eq. A20 of paper I,

$$\mathcal{F}(p, \zeta_o, Z_o) = {}_2F_1[a, 1-a; 1; \zeta_o] + \left(\frac{{}_2F_1[1+a, 2-a; 2; \zeta_o]}{{}_2F_1[1+A, 2-A; 2; Z_o]}\right) \times {}_2F_1[A, 1-A; 1; Z_o]. \tag{A7}$$

The definitions of a and A in Eqs. A5–A7 are given in Eqs. A14 and A15 of paper I.

Substituting Eq. A5 into A2, we have

$$\tilde{\eta}(p) = \frac{1}{p}\left[1 - \left(\frac{A_r + A_R}{A_R}\right)\frac{{}_2F_1[a, 1-a; 2; \zeta_o]}{\mathcal{F}(p, \zeta_o, Z_o)}\right] \tag{A8}$$

where A_r and A_R are the partial surface areas of the two cells (see Eqs. 6 and 7). We have now assembled almost all the results from paper I which are necessary to evaluate the limit in Eq. A8.

Note that in Eq. A8 the expression in brackets contains five hypergeometric functions. Each of these functions is expressible as a simple power series in p. The combining of these power series will produce a power series for the bracket in which the leading term contains a factor p which cancels the leading factor p^{-1} in Eq. A8. To complete the task of evaluating the limit of Eq. A8, we list the five power series in Eq. A9, correct through terms linear in p, which we require

$${}_2F_1[a, 1-a; 2; \zeta_o] = 1 + \frac{r^2 p}{D}\left[\left(\frac{1-\zeta_o}{\zeta_o}\right)\ln(1-\zeta_o) + 1\right] + \ldots \tag{A9}$$

$${}_2F_1[a, 1-a; 1; \zeta_o] = 1 - \frac{r^2 p}{D}\ln(1-\zeta_o) + \ldots \tag{A10}$$

$${}_2F_1[1+a, 2-a; 2; \zeta_o] = \frac{1}{1-\zeta_o}$$

$$+\frac{r^2p}{D}\left(\frac{1}{1-\zeta_o}\right)\left[\left(\frac{1-\zeta_o}{\zeta_o}\right)\ln(1-\zeta_o)+1\right]+\ldots \quad \text{(A11)}$$

$${}_2F_1[A, 1-A; 1; Z_o] = 1-\frac{R^2p}{D}\ln(1-Z_o)+\ldots \quad \text{(A12)}$$

$${}_2F_1[1+A, 2-A; 2; Z_o] = \frac{1}{1-Z_o}$$

$$+\frac{R^2p}{D}\left(\frac{1}{1-Z_o}\right)\left[\left(\frac{1-Z_o}{Z_o}\right)\ln(1-Z_o)+1\right]+\ldots \quad \text{(A13)}$$

After substituting Eqs. A9–A13 in Eq. A9, the expression for τ in Eq. 27 is obtained.

APPENDIX B. DERIVATION OF τ FROM THE TWO-STATE KINETIC APPROACH

In this approach, the cell-cell fusion problem is mapped onto a one-dimensional diffusive barrier-crossing problem involving a bistable entropic potential, for which the macroscopic phenomenological rate constants can be expressed in terms of microscopic quantities (16–18).

At first, let us consider the potential surface of a bistable state system shown in Fig. 5 *a* which has a barrier located at $x = 0$. The system (a molecule) is defined to be in state R when $-\infty < x < 0$ and in state r when $0 < x < \infty$. The macroscopic rate equations for this general chemical reaction are given in Eqs. 12 and 13 and their solutions in Eqs. 15–19. In the diffusive limit, the probability density that the system is at x at time t, $P(x,t)$, satisfies the Smoluchowski equation

$$\frac{\partial P(x,t)}{\partial t} = \frac{\partial}{\partial x} D(x) e^{-\beta U(x)} \frac{\partial}{\partial x}\left[e^{\beta U(x)} P(x,t)\right] \quad \text{(B1)}$$

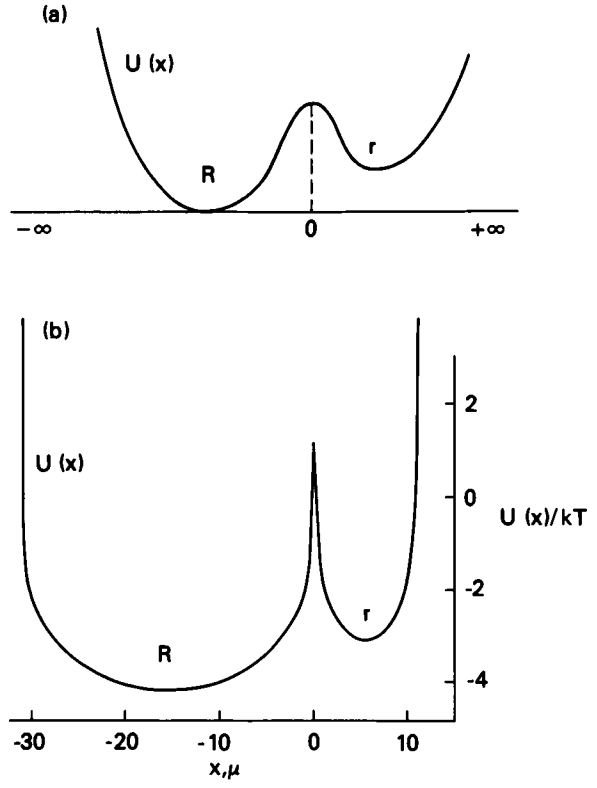

FIGURE 5 (*a*) Schematic drawing of a bistable potential in the barrier-crossing model of Kramers for a chemical reaction. (*b*) The calculated $U(x)$ (Eqs. B7 and B9) for a fusion complex of RBC ($r = 3.5$ μm) and Gp4f cells ($R = 10$ μm) at a pore size of $d = 0.05$ μm.

where $D(x)$ is a position-dependent diffusion coefficient and $\beta = (kT)^{-1}$. The equilibrium constant is determined by the potential $U(x)$:

$$K_{eq} = \frac{k_{R\to r}}{k_{r\to R}} = \frac{n_T(\infty)}{N_T(\infty)} = \frac{\int_0^\infty e^{-\beta U(x)}\,dx}{\int_{-\infty}^0 e^{-\beta U(x)}\,dx}. \quad \text{(B2)}$$

Microscopic expressions for the rate constants can be found by generalizing Kramers' (16) seminal work on diffusive barrier crossing. Using the theory of first-passage times (17), it can be shown that (18)

$$\tau = (k_{r\to R} + k_{R\to r})^{-1} = \left(\frac{N_T(\infty)}{n_T(\infty)+N_T(\infty)}\right) \times \frac{\int_0^\infty [D(x)e^{-\beta U(x)}]^{-1}\left[\int_x^\infty e^{-\beta U(y)}dy\right]^2 dx}{\int_0^\infty e^{-\beta U(x)}\,dx} + \left(\frac{n_T(\infty)}{n_T(\infty)+N_T(\infty)}\right) \times \frac{\int_{-\infty}^0 [D(x)e^{-\beta U(x)}]^{-1}\left[\int_{-\infty}^x e^{-\beta U(y)}dy\right]^2 dx}{\int_{-\infty}^0 e^{-\beta U(x)}\,dx}. \quad \text{(B3)}$$

Thus, τ and the individual rate constants $k_{r\to R}$ and $k_{R\to r}$ can be obtained from Eqs. B2 and B3.

We now return to the problem of primary interest, namely the diffusion of fluorescent probes on the surfaces of two fused cells shown in Fig. 1. As discussed in paper I, the surface densities of probes on the two cells obey the diffusion equations (12)

$$\frac{\partial n(\theta,t)}{\partial t} = \frac{D}{r^2}\frac{1}{\sin\theta}\frac{\partial}{\partial\theta}\left[\sin\theta\frac{\partial n(\theta,t)}{\partial\theta}\right], \qquad 0 \le \theta \le \theta_o \quad \text{(B4)}$$

and

$$\frac{\partial N(\Theta,t)}{\partial t} = \frac{D}{R^2}\frac{1}{\sin\Theta}\frac{\partial}{\partial\Theta}\left[\sin\Theta\frac{\partial N(\Theta,t)}{\partial\Theta}\right], \qquad 0 \le \Theta \le \Theta_o \quad \text{(B5)}$$

where D is the same position-independent diffusion coefficient of probes on each cell.

Let us introduce a new coordinate x defined as

$$x = R(\Theta - \Theta_o), \qquad 0 < \Theta < \Theta_o;$$
$$= r(\theta_o - \theta), \qquad 0 < \theta < \theta_o. \quad \text{(B6)}$$

Then a particle (probe) is on the R cell when $-x_R < x < 0$ and on the r cell when $0 < x < x_r$ where $x_r = r\theta_o$ and $-x_R = R\Theta_o$. Define a potential function $U(x)$ and a probability function $P(x,t)$ for particles on each cell as

$$U(x) = -kT\ln(2\pi R\sin\Theta), \quad \text{(B7)}$$

$$P(x,t) = e^{-\beta U(x)} \times N(\Theta,t), \qquad -x_R < x < 0; \quad \text{(B8)}$$

$$U(x) = -kT\ln(2\pi r\sin\theta), \quad \text{(B9)}$$

$$P(x,t) = e^{-\beta U(x)} \times n(\theta,t), \qquad 0 < x < x_r. \quad \text{(B10)}$$

Since $R\sin\Theta_o = r\sin\theta_o$, both $U(x)$ and $P(x,t)$ are *continuous* functions of x. Since $U(x)$ is proportional to T, it is an entropic potential (i.e., $U = -TS$, with $S = k\ln\Omega$ where Ω is the circumference of a circle with radius $R\sin\Theta$ or $r\sin\theta$). Note that with these definitions

$$n_T(t) = 2\pi r^2\int_0^{\theta_o} n(\theta,t)\sin\theta\,d\theta = \int_0^{x_r} p(x,t)\,dx \quad \text{(B11)}$$

and

$$N_T(t) = 2\pi R^2\int_0^{\Theta_o} N(\Theta,t)\sin\Theta\,d\Theta = \int_{-x_R}^0 P(x,t)\,dx. \quad \text{(B12)}$$

The effective entropic potential $U(x)$ evaluated for the fusion complex of RBC and Gp4f cells with a pore size of 0.05 μm shown in Fig. 5 *b*.

Using Eqs. B6–B10, the two diffusion equations in Eqs. B4 and B5 can be combined in a single equation that has the same form as Eq. B1 with $D(x) = D$. That is, the diffusion of particles on the composite surface of the

fusion complex in Fig. 1 is equivalent to the one-dimensional diffusion of particles on a bistable potential defined by Eqs. B7 and B9 (see Fig. 5, *a* and *b*). Thus, the general expression in Eq. B3 reduces in our application to

$$\tau = (k_{r\to R} + k_{R\to r})^{-1}$$
$$= \left(\frac{A_R}{A_r + A_R}\right)\left(\frac{r^2}{D}\right)\frac{\int_0^{\theta_0}\frac{d\theta}{\sin\theta}\left(\int_0^{\theta}\sin\theta'\,d\theta'\right)^2}{\int_0^{\theta_0}\sin\theta\,d\theta}$$
$$+\left(\frac{A_r}{A_r + A_R}\right)\left(\frac{R^2}{D}\right)\frac{\int_0^{\Theta_0}\frac{d\Theta}{\sin\Theta}\left(\int_0^{\Theta}\sin\theta'\,d\theta'\right)^2}{\int_0^{\Theta_0}\sin\Theta\,d\Theta}. \quad \text{(B13)}$$

Evaluating the integrals, we obtain the expression for τ in Eq. 27.

APPENDIX C. EVALUATION OF THE VALUE OF κ IN EQ. 10

In this appendix, we discuss how to estimate the value of κ in Eq. 10 for nonlinear-quenching fluorophores from the data in Fig. 1 of Aroeti and Henis (13), in which the degree of quenching of R-18 from nonfusion vesicles is plotted as a function of the R-18 density. As shown in the figure, the concentration dependence of quenching of R-18 molecules may be linear or nonlinear, depending on the lipids used in the measurements. We consider only the nonlinear case.

The degree of quenching of R-18 at density n, Q_n, is defined as the fractional decrease in specific fluorescence due to self-quenching:

$$Q_n = \frac{f[0] - f[n]}{f[0]} \quad \text{(C1)}$$

where $f[0]$ and $f[n]$ are the specific fluorescences of an R-18 molecule at densities zero (infinite dilution) and n, respectively. After substituting with Eq. 10, Eq. C1 becomes

$$Q_n = \frac{\kappa n}{1 + \kappa n}. \quad \text{(C2)}$$

Eq. C2 can be rearranged as

$$\frac{1}{Q_n} = 1 + \left(\frac{1}{\kappa}\right)\left(\frac{1}{n}\right). \quad \text{(C3)}$$

Thus, a plot of $1/Q_n$ against $1/n$ yields a slope equal to $1/\kappa$. From the nonlinear curve in Fig. 1 of Aroeti and Henis (13), the value of κ was estimated to be 2/unit mole% of R-18.

We would like to thank Dr. Robert Blumenthal for valuable discussions.

REFERENCES

1. Okada, Y. 1988. Sendai virus-mediated cell fusion. *Curr. Top. Membr. Transp.* 32:297–336.
2. White, J. M. 1990. Viral and cellular membrane fusion proteins. *Ann. Rev. Physiol.* 52:675–697.
3. Hoekstra, D., T. de Boer, K. Klappe, and J. Wilschut. 1984. Fluorescence method for measuring the kinetics of fusion between biological membranes. *Biochemistry.* 23:5675–5681.
4. Hoekstra, D., and K. Klappe. 1986. Use of a fluorescence assay to monitor the kinetics of fusion between erythrocyte ghosts, as induced by Sendai virus. *Biosci. Rep.* 6:953–960.
5. Loyter, A., V. Citovsky, and R. Blumenthal. 1988. The use of fluorescence dequenching methods to follow viral membrane fusion events. *Methods Biochem. Anal.* 33:128–164.
6. Blumenthal, R., A. Bali-Puri, A. Walter, D. Covell, and O. Eidelman. 1987. pH-dependent fusion of vesicular stomatitis virus with vero cells: measurement by dequenching of octadecylrhodamine fluorescence. *J. Biol. Chem.* 262:13614–13619.
7. Puri, A., J. Winick, R. J. Lowy, D. Covell, O. Eidelman, A. Walter, and R. Blumenthal. 1988. Activation of vesicular stomatitis virus fusion with cells by pretreatment at low pH. *J. Biol. Chem.* 263:4749–4753.
8. Sarkar, D. P., S. J. Morris, O. Eidelman, J. Zimmerberg, and R. Blumenthal. 1989. Initial stages of influenza hemagglutinin-induced cell fusion monitored simultaneously by two fluorescence events: cytoplasmic continuity and lipid mixing. *J. Cell Biol.* 109:113–122.
9. Morris, S. J., D. P. Sarkar, J. M. White, and R. Blumenthal. 1989. Kinetics of pH-dependent fusion between 3T3 fibroblasts expressing influenza hemagglutinin and red blood cells. *J. Biol. Chem.* 264:3972–3978.
10. Kaplan, D., J. Zimmerberg, A. Puri, D. P. Sarkar, and R. Blumenthal. 1991. Single cell fusion events induced by influenza hemagglutinin: studies with rapid-flow, quantitative fluorescence microscopy. *Exp. Cell Res.* 195:137–144.
11. Chen, Y., and R. Blumenthal. 1989. On the use of self-quenching fluorophores in the study of membrane fusion kinetics; the effect of slow probe redistribution. *Biophys. Chem.* 34:283–292.
12. Rubin, R. J., and Y. Chen. 1990. Diffusion and redistribution of lipid-like molecules between membranes in virus-cell and cell-cell fusion systems. *Biophys. J.* 58:1157–1167.
13. Aroeti B., and Y. I. Henis. 1987. Fusion of native Sendai virions with human erythrocytes. Quantitation by fluorescence photobleaching recovery. *Exp. Cell Res.* 170:322–337.
14. Zhou, H-X., and R. Zwanzig. 1991. A rate process with an entropy barrier. *J. Chem. Phys.* 94:6147–6152.
15. Zwanzig, R. 1992. Diffusion past an entropy barrier. *J. Phys. Chem.* 96:3926–3930.
16. Kramers, H. A. 1940. Brownian motion in a field of force and the diffusion model of chemical reactions. *Physica.* 7:284–304.
17. Szabo, A., K. Schulten, and Z. Schulten. 1980. First passage time approach to diffusion controlled reactions. *J. Chem. Phys.* 72:4350–4357.
18. Schulten, K., Z. Schulten, and A. Szabo. 1981. Dynamics of reactions involving diffusive barrier crossing. *J. Chem. Phys.* 74:4426–4432.